EXPERIMENTAL AND NUMERICAL ANALYSIS OF REPAIRED STIFFENED CFRP PANELS UNDER COMPRESSION

Dalong Dong[1], Hai Wang[1] and Xiang Zhou[1,*]

[1]School of Aeronautics and Astronautics, Shanghai Jiao Tong University
800 Dongchuan Road, Shanghai, China
[*]Email: xiangzhou@sjtu.edu.cn

Keywords: stiffened CFRP panel, structural repair, experiment, numerical analysis, mechanical properties

Abstract

Carbon Fiber Reinforced Plastics (CFRP) stiffened panels have been widely used in the aerospace industry due to their high strength and stiffness. However, this type of structure is also susceptible to impact damage. Therefore, the study on various repair methods of the damaged CFRP is of paramount importance because the repaired structures can recover an acceptable level of functionality. This paper presents an experimental and numerical study on the mechanical behaviors of CFRP stiffened panels containing two types of initial defects with three repair methods i.e. mechanical repair, adhesively bonded repair and scarf patch repair. The experimental specimens were tested in compression and the material used were carbon fibre/epoxy composite. The finite element method was employed to simulate the compressive loading procedure. For most cases, both the panel and the stringers are meshed with S4R elements and the Hashin damage criteria is used to determine element failure. The FE modelling protocol was then verified through comparison between the experimental and simulation results and a good agreement between them was attained. The results illustrated in this work can provide researchers and engineers with a general guideline on the selection of the most appropriate repair methods for certain damage type.

1. Introduction

Carbon Fiber Reinforced Plastics (CFRP) is widely used in industrial sectors such as aviation, construction, wind energy and transportation due to its high weight-specific mechanical strength and stiffness. In particular, stringer-stiffened CFRP panels are a genre of structures which substantially enhance the composites' mechanical properties at the cost of very small increase in weight. Moreover, the stiffened structures are convenient to manufacture and install. Therefore, they have become a typical structural component widely used in aerospace engineering such as the wall panel of wing and empennage, the bulkhead of fuselage and so on. When being used in practical structures, however, composites are inevitably subjected to impacts, which can cause serious damage within certain area of the panel and lead to catastrophic failure. As bigger and more important components are manufactured from composites, the problems on their damage and repair become more critical.

A lot of work has been carried out on repair problems associated with various defects. Riccio[1] study the delamination buckling growth of a CFRP stiffened panel by a series experiment. Generally, there are two types of structural repair methods, namely adhesively bonded structural repair (ABSR) and mechanically fastened structural repair (MFSR) [2]. Some authors such as Hart-Smith [3], Heslehurst [4], and Robson [5] tend to use MFSR for field repairs, thick monolithic structures and highly loaded structures, whereas ABSR should be used for structures under light to moderate loads and thin structures. Hart-Smith [3] proposed that MSFR provides better mechanical performances than ABSR

Excerpt from ISBN 978-3-00-053387-7

at all times if sufficient thought on repair ability is given at the design stage. However, Myhre and Beck [6] put the opposite argument in favor of ABSR if fibre reinforced composite is bonded in nature. It is worth noting that MFSR are incompatible with sandwich structures [7]. Thus far, there are no generally agreed conditions in the literature about which one is the better choice for composite structural repair, leading to an experience-based design methodology for the determination of repair strategies [5]. In the field of experimental study, Bredmose [8] performed experimental investigations on steel adhesive double lap joints (DLJ) reinforced by rivets. The experiments using the Digital Image Correlation (DIC) system allows for exact monitoring of the deformation process of the considered hybrid joint. Several analytical approaches have also been developed for the design and evaluation of repair techniques. In the specific case of ABSR, the calculations on the repair joint design were based on the work by Hart-Smith on adhesive bonded joints [10,11]. Similar work by the same author has been conducted for MFSR, namely bolted and riveted repairs. The code developed from these solutions was also incorporated in a composite repair expert system developed by Sandow [12].

While the finite element (FE) method has been widely used in the development of new composite structures, there is a relative rarity in literatures directly dealing with the FE modelling of composite structure repairs [13-15]. Soutis and Hu [16, 17] have shown that the traditional 2D plane strain models used for bonded joints were not entirely suitable to represent accurately externally bonded repairs to composite panels and suggested that a full 3D model using solid elements with equivalent orthotropic properties be used to study the adhesively bonded repair. The same approach[18] was used to a 3D model in the study of scarfed repairs, in which the FE results agreed well with the experimental data, revealing that the optimum scarf angle was around 7° compared to 4° predicted previously by a 2D model. Baker et al [19] used a detailed 3D FE model to investigate scarf repairs on carbon epoxy components. In this study, each ply in the structure was modelled individually as separate elements. Good agreement was obtained between the FE and experimental results for strains.Riccio[20] use the VCCT techinique to study the delamination growth in FEM. Bredmose[8] investigated a 3D model for mechanically repair joints, adhesively bonded and hybrid joints with a cohesive zone which was convenient for the description of the adhesive and hybrid joints. The numerical results compare well with the experimental data.

The present work aimed to compare the mechanical properties of stiffened CFRP panels with various damages and repair methos subjected to compression . An experimental and numerical study were performed to fulfill this goal. In experiments, the ultimate strength and failure mode were evaluated for various specimens with or without repair. The numerical analysis was performed in ABAQUS and the simulation results were validated with experimental results. The FE analysis allowed obtaining the deformation pattern, failure mode including the debongding path , which provided further insight into the repair behavior.

2. Experimental study

2.1. Test specimens

Each test specimen consists of a 308×300 mm panel and four equally-distributed T-shaped stiffeners, as shown in Fig. 1 The panel is made from 25 plies of unidirectional carbon/epoxy prepreg with the stacking sequence $[45/-45/0/-45/45/0/-45/45/90/45/-45/45/0]_s$, leading to a thickness of about 3 mm. The web and flange of the stiffeners comprise respectively 27 and 17 plies of the same unidirectional prepreg as the panel in a quasi-isotropic lay-up. The stiffeners are bonded onto the panel using an epoxy-based structural adhesive. Both end sections of the specimen extending 40 mm from the edge are reinforced by a resin block wrapped inside a metal case to provide stability during the experiment.

Three types of defects, referred to as D1 to D3, are considered, where D1 and D2 denote panel delaminations of size 35×90 mm between the twelveth and thirteenth plies and between the sixth and seventh plies, respectively, D3 denotes stiffener debond that extends 90 mm along the stiffener. In

Excerpt from ISBN 978-3-00-053387-7

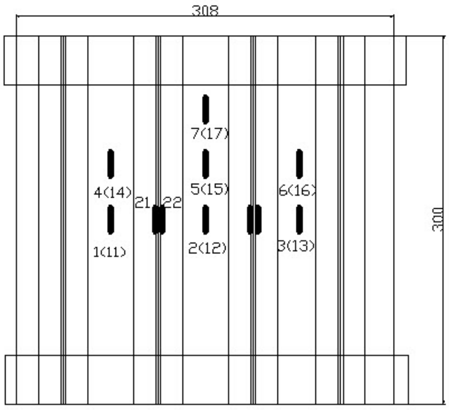

(a)

(b)

Figure 1. The geometry of the specimen and the arrangement of strain gages: (a) front view; (b) cross-section view.

addition, the combination of defects D1 and D2 and that of D2 and D3 are considered, referred to as D12 and D23, respectively.

Three repair methods, namely mechanical repair (MR), adhesively-bonded repair (ABR) and scarf patch repair (SPR), are investigated in this paper where the MR and ABR methods are applicable to all five defect types mentioned above and the SPR method is only applied to D1 or D2. In the MR method, the delamination or debond region is strengthened by ten equally-distributed steel rivets. In the ABR method, a patch made from 5 plies of the same unidirectional prepreg as the panel with the stacking sequence [45/-45/0/-45/45] is bonded to the back side of the panel (i.e. the side without stiffeners) using the same epoxy-based structural adhesive that bonds the stiffeners to the panel. In the SPR method, the plies between the delamination layer and the back side of the panel are removed and a scarf patch made from the same unidirectional prepreg as the panel is filled into the dent . For defect types D1 and D2, the scarf patchs comprise 14 and 8 plies with the stacking sequences [45/-45/45/-45/0/-45/45/0/-45/45/90/45/-45/45] and [45/-45/45/-45/0/-45/45/0], respectively. The experiment matrix is shown in Table 1. For each case, three specimens are tested. In addition, specimens that are unrepaired (UR) are also tested for comparison.

2.2 Experimental setup

Edgewise compression tests with the specimens listed in Table 1 were performed. In the test, each specimen was placed between the flat load platens mounted on a MTS C64.106 materials testing machine (MTS Systems, USA), as shown in Fig. 2 and compressed at a constant crosshead rate of 1

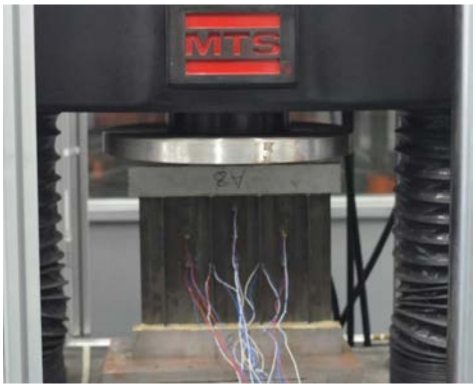

Figure 2. The experimental setup.

Excerpt from ISBN 978-3-00-053387-7

Table 1. The matrix for the test specimens

	D1	D2	D3	D12	D23
unrepaired (UR)	3	3	3	3	3
mechanical repair (MR)	3	3	3	3	3
adhesively-bonded repair (ABR)	3	3	3	3	3
scarf patch repair (SPR)	3	3			

mm/min along the longitudinal direction of the stiffener until a 30% drop in the load was recorded, indicating that the failure of the specimen occurred. During the test, the specimen were instrumented with eighteen back-to-back strain gages in skin and stringer locations, as shown in Fig. 1 and the strain-load data were recorded using a VTI EX1629 digital acquisition system (VTI Instruments, USA).

2.3 Experimental Result

The ultimate compressive strength per unit weight of the test specimens are shown in Fig. 3. According to the results, panel delaminations have greater influence on the residual strength of the unrepaired specimens than stiffener debond does, and the residual strength appears to be insensitive to where the delamination locates. For specimens involving panel delamination defects, all three repair methods restore the strength of the defective specimens to some extent and the ABR method is the most effective one. For the stiffener debond defect, however, the MR method appears to be the only effective repair method whereas the ABR method even reduces the compressive strength of the specimen.

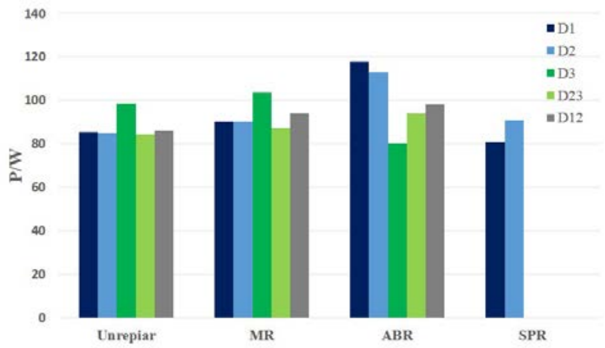

Figure 3. The summary of static test result.

3. FE simulations

3.1 FE modeling method

In this paper, the FE analysis was performed in the FE package ABAQUS/Explicit (SIMULIA Inc., USA). Five numerical models M1 to M5 were considered, where M1 and M2 are the unrepaired cases with defect types D1 and D3, respectively, and M3 to M5 are cases with defect type D1 that are repaired with the MR, ABR and SPR methods, respectively. In general, the panel and the stiffeners are meshed with 4-node reduced integration shell elements (S4R) and the adhesive layer between the panel and the stiffener is meshed with 8-node three-dimensional cohesive elements (COH3D8). In case of panel delamination, the panel is meshed with two layers of S4R elements connected by a third layer of COH3D8 elements with a rectangular cut defining the delamination region, as shown in Fig. 4(a). In case of stiffener debond, the elements in the debond region in the adhensive layer are deactivated, as shown in Fig. 4(b). In case of the MR method, the rivets and the panel are modelled with fastener elements and S4R respectively. In case of the ABR method, the patch and the adhesive

Excerpt from ISBN 978-3-00-053387-7

layer between the patch and the panel are meshed with S4R and COH3D8 elements, respectively. Finally, in case of the SPR method, the scarf patch and the adhesive layer are modelled with fastener S4R and COH3D8 respectively (as shown in Fig. 4(d)). A plane stress orthotropic elastic material model with the Hasin failure criteria was employed to simulate the unidirectional carbon/ material. The Linear Power Law was employed to simulate the adhesive layer delamination growth. The material properties used in the simulations are summarized in Table 2.

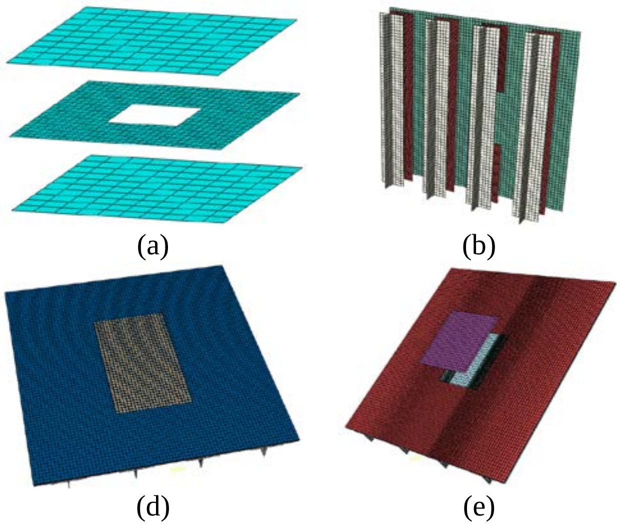

Figure 4. (a) The FEM model of M1 ; (b) The FEM model M2; (c) The FEM model M3; (d) The FEM model M4; (e) The FEM model M5

Table 2. The material properties used in the simulations

E_{11} / GPa	E_{22} /GPa	G_{12} /GPa	ν_{12}
126	10.7	4.47	0.33

3.2 Validation of the FE models

Virtual compression tests with the specified five FE models were performed. Because both ends of the test specimen are strengthed with resin, the strengthened regions can be considered as being rigid and thus excluded from numerical models for simplicity. To simulate the compressive loading, the nodes at one cutting end of the panel were fixed both translationally and rotationally and the nodes in the opposite cutting end were displaced towards the constrained end. The ultimate compressive strengths of the five models obtained from the physical and virtual tests are listed in Table 3. A good agreement between the FE and experimental results can be observed, indicating the validity of the FE models.

Table 3. The ultimate strength of experiment and FEM

Model	Ultimate strength, Exp. (kN)	Ultimate strength, FE (kN)	Error(%)
M1	442.5	437.8	1.1
M2	644.4	623.2	3.3
M3	585.6	548.6	6.3
M4	772.7	694.3	10.2
M5	567.6	552.5	2.6

3.3 Analysis of failure modes

Excerpt from ISBN 978-3-00-053387-7

Figure 5 illustrated the deformed shapes and delamination and debond growth path from the FE simulations. In M1, there is a small upwarp because of the skin delamination and themaximum of the out-plane displacement is 3.90 mm (Fig. 5(a). The upwarp leads to local buckling and delamination growth (Fig. 5(b)). The fracrure load and destructive displacement reach buckling and delamination

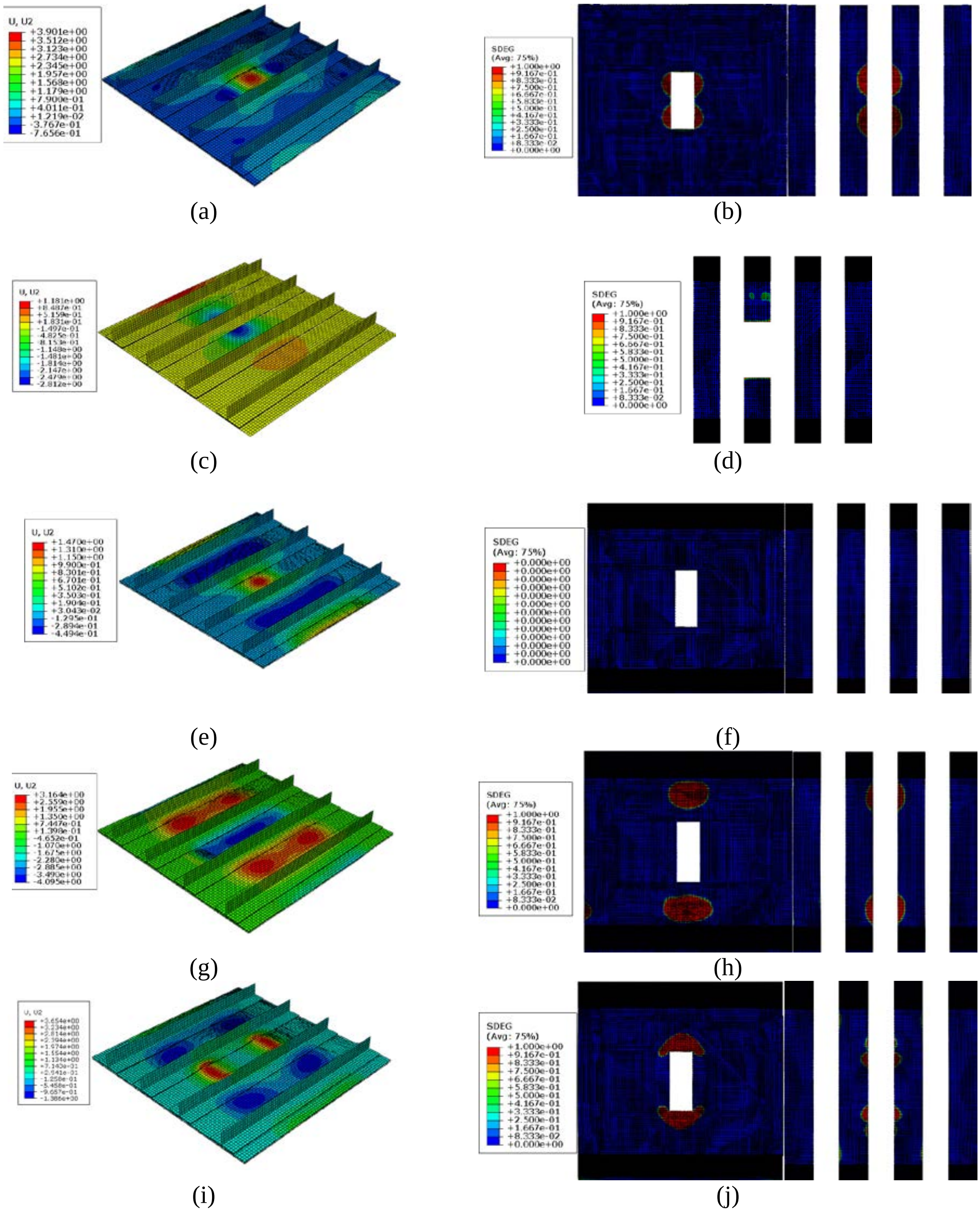

Figure 5. (a) Deformed shapes of M1 under fracture load; (b) Delamination and debond growth path of M1; (c) Deformed shapes of M2 under fracture load; (d) Delamination and debond growth path of M2; (e) Deformed shapes of M3 under fracture load; (f) Delamination and debond growth path of M3; (g) Deformed shapes of M4 under fracture load; (h) Delamination and debond growth path of M4; (i) Deformed shapes of M5 under fracture load; (j) Delamination and debond growth path of M5.

growth (Fig. 5(b)). The fracrure load and destructive displacement reach buckling and delamination growth (Fig. 5(b)). The fracrure load and destructive displacement reach 442.5 kN and 1.86mm respectively. In M2, the local buckling occurred at the disbond area but the out-plane displacement reaches 2.48 mm when the strcture bears the largest load. There is sunken skin instead upwarp because of the disbond (Fig. 5(c)). The disbonds growth is not obvious though (Fig. 5(d)). The fracrure load and destructive displacement reach 623.2 kN and 1.58 mm, respectively. In M3, there is a local buckling occurred at the skin delamination area but the out-plane displacement decrease to 2.76 mm when the strcture bears the largest load compared to M1 (Fig. 5(e)). A delamination growth has propagaten along both longitudinal and transvese direction (Fig. 5(f)). The structural-load-carrying capacity can be enhanced because of mechanically fastened structural repair. The fracrure load and destructive displacement reach 548.7 kN and 1.85 mm, respectively. In M4, there is a local buckling occurred at the skin delamination area but the out-plane displacement decrease to 2.62 mm when the strcture bears the largest load. However, the dimension of local buckling area has increased compared to the M1 and M3 (Fig. 5(g)). No delamination growth occurred but the disbond generated at stiffeners (Fig. 5(h)). The fracrure load and destructive displacement reach 694.3 kN and 1.75 mm respectively. Finally, in M5, the local buckling occurred at the skin delamination area but the out-plane displacement decrease to 2.48 mm when the strcture bears the largest load. There are two upwarp at the skin which is different compared to the deformation pattern mentioned above (Fig. 5(i)). A delamination growth has propagaten from the edge of the delaminaton area along both longitudinal direction only(Fig. 5(j)). The fracrure load and destructive displacement reach 552.5 kN and 2.51 mm, respectively.

4. Conclusions

In this paper, an experimental and numerical study was performed on stiffened CFRP panels containing damage with various repair methods under compressive loading. Several conclusions can be drawn from the experimental results. First, panel delaminations have greater influence on the residual strength of the unrepaired specimens than stiffener debond does. For specimens involving panel delamination defects, all three repair methods restore the strength of the defective specimens to some extent and the ABR method is the most effective one. Finally, for the stiffener debond defect, however, the MR method appears to be the only effective repair method whereas the ABR method even reduces the compressive strength of the specimen. FE modelling techniques for vaious damage types and repairs methods were also developed and validated through the experimental results. Moreover, a detailed analysis on the failure modes of the specimens under compression was discussed based on the simulation results. This work provides a solid foundation for the future parameter analysis and optimization of the mechanical performances of damaged CFRP panels with various repair methods.

References

[1] Riccio. Delamination buckling and growth phenomena in stiffened composite panels under compression. Part I: An experimental study. *Journal of Composite Materials*, 48.23: 2843-2855,2014.
[2] T.N. Cook, M. Renieri, G. B. Breault, and R.Cox. Advanced composite structures R&M design and repair guide. USAACOM Report No. TR-85-D-12, USA, 5.1–5.5,1986.
[3] L.J. Hart-Smith. *Adhesively Bonded Joints for Fibrous Composite Structures*. *Recent Advances in Structural Joints and Repairs for Composite Materials*. Springer Netherlands, 2003.
[4] R.B. Heslehurst. Analysis and modelling of damage and repair of composite materials in aerospace. Springer Netherlands, 1996.
[5] J.E. Robson. The repair of composite materials. Diss. Ph. D. thesis, Centre for Composite Materials. Imperial College of Science Technology and Medicine, University of London, 1993.

Excerpt from ISBN 978-3-00-053387-7

[6] S.H. Myhre and C. E Beck. Repair concepts for advanced composite structures. *Journal of Aircraft*, 16:720–728, 1979.

[7] R.E.Trabocco, T.M. Donnellan, and J. G. Williams. *Repair of composite aircraft. Bonded Repair of Aircraft Structures*. Springer Netherlands, 1988.

[8] H. Bredmose, M. Brocchini, D.H. Peregrine, and L. Thais. Experimental investigation and numerical modelling of steep forced water waves. *Journal of Fluid Mechanics*, 490: 217-249, 2003.

[9] S.R. Hall, M.D. Raizenne, and D.L. Simpson. Aproposed composite repair methodology for primary structures. *Composites*, 20:479–483, 1989.

[10] L.J. Hart-Smith. Analysis and design of advanced composite bonded joints. NASA contractor Report CR-2218, 1974.

[11] L J. Hart-Smith, Adhesive bonded scarf and stepped lap joints, NASA Contractor Report CR 112237, 1973.

[12] F.Sandow. A computer aided aircraft structural composite repair system. *Proceedings 32nd International SAMPE Symposium*, 1987.

[13] Odi, A.Randolph, and Clifford M. Friend. A comparative study of finite element models for the bonded repair of composite structures. *Journal of reinforced plastics and composites.* 21(4):311 332, 2002.

[14] K.Loss, and K. Kedward. Modeling and analysis of peel and shear stresses in adhesively bonded Joints. *25th Structures, Structural Dynamics and Materials Conference*, 1984.

[15] M.P. Siener. Stress field sensitivity of a composite patch repair as a result of varying patch thickness. *Composite Materials: Testing and Design*, 1992.

[16] C. Soutis and F.Z. Hu. Design and performance of bonded patch repairs of composite structures. *IMechE Conference on Airworthiness Aspects of New Technologies*, Bristol, UK, November 10, 1996.

[17] C. Soutis and F.Z. Hu. Repair design of composites and efficiency of scarf patch repairs. *Proceedings 11th International Conference on Composite Materials,* July, 1997.

[19] A.A. Baker, R.J. Chester, G.R. Hugo, and T.C. Radtke. Scarf repairs to graphite/epoxy components. AGARD-CP-550, 19.1–19.12, 1995.

[20] Riccio. Delamination buckling and growth phenomena in stiffened composite panels under compression. Part II: a numerical study. *Journal of Composite Materials,* 46: 2843-2855,2013.

Excerpt from ISBN 978-3-00-053387-7